Comparing Apparent Haptic Motion and Funneling for the Perception of Tactile Animation Illusions on a Circular Tactile Display

Thomas Pietrzak (ID) and Rahul Kumar Ray (ID)

Abstract—Tactile animation illusions are used to display dynamic information with haptic cues. In this study, we investigate two forms of tactile animation illusions that leverage the Funneling effect and Apparent Haptic Motion (AHM) on a one-dimensional circular tactile display. We define new parameters for the description of AHM that describe both the temporal and spatial aspects of these animations: Angle per Actuator (APA) and Revolution Duration (RD). We present three user studies about the perception of angular animations produced with these effects. Our results show that people can interpret AHM animations regardless of the APA value and that they can interpret tactile animation illusions slower than one degree per second. We also showed that the participants' ability to discriminate angular animations improves proportionally with the angle presented.

Index Terms—Apparent Haptic Motion, Haptic Illusions, Tactile Funneling, Tactile Display, Tactile Illusion, Tactile Animation Illusion, Phantom Sensation, Phantom Motion

I. INTRODUCTION

TACTILE animation illusions leverage the sense of touch to create the illusion of haptic cues moving on the body surface. A straightforward way to create tactile animation is a sequence of actuations at different body locations [2], [6], [28], [50]. However, compared to a simple sequence of actuations, more elaborate tactile animations can give a smoother and continuous illusion. For example, in this study we focus on the comparison of two such tactile animations: *Apparent Haptic Motion* (AHM) [45] and *Funneling* also known as *Phantom sensations* [5]. AHM is generated through a series of vibrations with an overlap in activation. The *Funneling* effect gives the illusion of a virtual vibration in between two actuators by interpolating their amplitude of actuation. The movement illusion is created by moving around this virtual vibration.

AHM offers the advantage of operating with a simple on/off signal, allowing even basic actuators like eccentric rotating mass (ERM) to produce this effect accurately. However, voice coil actuators, which give precise control over signal amplitude [30], can cover a larger range of parameters [33] of AHM and are required for an accurate rendering of the funneling effect. The benefit of funneling lies in establishing a bijection between the command and the position of the resulting virtual vibration. This proves useful, for instance, in creating a tactile display with a tactile cursor that the user can move around with direct manipulation [10].

Circular tactile displays hold great potential for haptic interaction, particularly in the context of wrist-worn devices like smartwatches [10], [28], [39] since it relies on augmenting existing devices. Despite their significance, circular animations employing these techniques have received comparatively less attention in the literature. Our research aims to address this gap, exploring the perception of circular AHM and funneling animations.

In the literature about circular AHM animations, several studies have explored just noticeable differences (JND) in animation speed. Kohli *et al.* used five voice coil actuators around the arm [19], the objective was to create a set of distinguishable animations. Ogrinc *et al.* used six ERM actuators to establish a speed threshold for correctly identifying animations and design Tactons by combining speed and amplitude [34]. Additionally, a study comparing circular displays with varying numbers of voice coil actuators between three and five and found that four actuators were sufficient for participants to feel AHM animations over a wide range of parameters [32]. Building upon this foundational research, our work aims to extend the investigation to a comparative analysis between AHM and funneling animations, specifically focusing on establishing JND for angle animations. Two other studies studied the perception of the funneling effect with circular tactile displays based on ERM actuators. Hong *et al.* compared the identification of funneling cues around the arm with three, four, and five actuators [13]. They concluded that four actuators are enough to interpret accurately static angles created with a funneling effect. Luzhnica *et al.* used four actuators and proposed a new interpolation method considering the differences in touch sensitivity across actuator locations on the body [27]. While these two studies focused on static angle representations, our contribution lies in exploring the dynamic nature of angular animations. The only study we are aware of that studied circular funneling animations with voice coil actuators focused on direct manipulation of the phantom sensation for the design of a tactile display [10]. The objective of our work is rather tactile animation illusions not controlled by the user. Previous work combined AHM and the funneling effect to create tactile animation illusions [15].

Thomas Pietrzak is with the Université de Lille, France (e-mail: Thomas.Pietrzak@univ-lille.fr).

Rahul Kumar Ray is with FLAME University, Pune, India (e-mail: rahul-raiecb@gmail.com).

However, regardless of the device layout, we are unaware of any study comparing AHM and funneling animations.

We present the design of two haptic prototypes used in our experiments, featuring different layouts of actuators. Additionally, we elaborate on the haptic signal, introducing new parameters of AHM that characterize both the spatial and temporal aspects of tactile animations and allow an easier comparison with the funneling effect. Lastly, we present findings from three user studies. The first study examines the impact of these new parameters on users' ability to interpret AHM animations. The second experiment compares users' proficiency in interpreting AHM and funneling animations using the two layouts. In the third study, we determine the angle discrimination threshold for both AHM and funneling, considering reference angles ranging from 90° to 360°.

II. RELATED WORK

Tactile animations can be simply created by activating several actuators in a sequence, eventually with pauses between the vibrations [6]. Several body locations are suitable, in particular the hand palm [2], [50] and the wrist [28], [35]. However, this method gives a discrete sensation as opposed to a sensation of a vibration moving continuously across the body surface.

Lederman and Jones review a number of studies about haptic illusions [23]. In particular, they report a *movement illusion*: Tactile Apparent Motion, or Apparent Haptic Motion (AHM) [45]. They also mention two *errors of localization* illusions. The first one is the saltation effect, created with a series of short vibrations repeated at successive locations on the movement path, making it feel like the vibrations are moving along that path [9], [47]. The second one is the funneling effect, which leverages the property that two close tactile stimulations are felt as a virtual one in between them [5]. Animations are created by adjusting the position of the virtual vibrations over time.

AHM and the funneling effect can both create a smooth and continuous animation sensation, hence we focus on these tactile animation illusions in this study. Understanding the nuances between AHM and the funneling effect is crucial for developing effective haptic feedback systems.

A. Apparent Haptic Motion

Inspired by work on visual perception, Sherrick and Rogers investigated the perception of tactile animation with overlapping stimulations [45]. They experimented on the effect of the *Inter-Stimulus Onset Interval* (ISOI), also called *Stimuli Onset Asynchrony* (SOA), and *Stimulus Duration* (SD), also called *Duration of Signal* (DoS)[1]. They asked the participants to adjust the SOA to estimate the *"longest uninterrupted feeling of movement between the first stimulus site and the second"*. They observed that the participants chose SOA values smaller than DoS, hence with an overlap between successive actuations. The participants also reported that *"At*

[1]In this paper we use the SOA and DoS terms as they are standard in the current literature.

its best, the feeling was equivalent to that produced by actually moving a vibrating object smoothly [...]." Further studies confirmed that SOA and DoS both influence the feeling of an apparent motion [8], [14], [18]. The results suggest that the distance between actuators does not affect the sensation of continuous motion [8], [18], neither does the frequency of the signal [14]. Interestingly, the actuators do not have to use the same frequency to induce the AHM effect [16]. The AHM effect can also be transmitted between users wearing a haptic bracelet when they shake their hand [12]. While vibrations are the most common way to produce the effect, it can also be achieved using taps [21] or even thermal feedback [29]. Additionally, combining vibrotactile AHM with static thermal feedback can create the sensation of a moving hot spot [46].

Since the actuators are always positioned at fixed locations, adjusting the SOA and DoS parameters modifies the animation speed. Studies show that the speed discrimination threshold is inversely proportional to SOA, which is expected because the animation speed is inversely proportional to SOA [20]. The animation speed depends also on DoS though, therefore even if these parameters are convenient for the implementation of AHM animations, they are not convenient for designing animations. Hence, we propose new parameters for this purpose.

AHM studies used several body locations such as the arm [19], [32], [33], the hand [12], [40], the wrist [19], [32], [34], the fingers [20], [42], the legs [45], or the back [14]. However, previous studies on tactile perception observed large discrepancies in terms of tactile perception across the body [49]. The focus of our study is to create AHM effects around the wrist and compare them to funneling effects.

B. Funneling

The funneling effect was first discovered by von Békésy while studying the similarities between the perception of hearing and touch [4]. He described this effect as the simultaneous summation and inhibition of tactile signals from mechanoreceptors [5]. When the skin is stimulated simultaneously at two locations, the tactile sensation is perceived in between, creating what von Békésy calls a *phantom sensation*. Early research focused on the precision of stimulation localization and proposed a logarithmic interpolation model to equalize the apparent loudness between actuators [1]. More recent studies have compared various models, leading to the design of a model that accounts for the differences in tactile sensitivity across the skin surface [27].

Unlike AHM, the funneling effect is a stationary illusion. However, animations can be created by moving the phantom vibration over time. Initial work explored this concept between two points [7], and later studies extended this to longer distances, such as along the arm, using more actuators [3]. By allowing the user to control the phantom vibration, it is therefore possible to create tactile displays with direct manipulation capabilities [10].

While the aforementioned studies utilized 1D displays, 2D models have also been developed. For instance, amplitude interpolation between three actuators can produce a phantom sensation at any point within the triangle formed by those

actuators [48]. Another 2D model combines AHM and the funneling effect to create animations on an array of actuators placed on the back [15]. This model enables animations to follow a straight path on the 2D grid, with phantom sensations occurring between the actuators. Additionally, another approach merges the two methods to generate arbitrary trajectories on the hand [37]. A simpler model, which tiles the 2D surface with three-actuator patterns, has been employed to design a multisensory hand-held VR controller capable of producing tactile animations on the hand palm [41].

The funneling effect has been studied across various body locations, including the palm of the hand [37], [38], [48], the forearm [1], [3], [5], the fingers [38], the back [15], [44], the wrist [10], [13], [27], the head [17], and the legs [26]. Additionally, some studies have compared the effects of funneling across different body locations [22], [36]. In this study, we focus on 1D circular funneling animations on the wrist. While previous research has explored the recognition of static angles [13], [26], our work investigates animations, particularly in comparing AHM and the funneling effect.

Both AHM and the funneling effect are pivotal in creating smooth, continuous tactile animations. While AHM relies on overlapping stimulations [45], the funneling effect leverages simultaneous stimulations to generate a phantom sensation between two points [5] either as a static point or an animation. Despite their different mechanisms, both techniques have been extensively studied across various body locations, including the wrist, where our study is focused.

While prior research has explored static angle recognition on the wrist [13], [26], there has been limited exploration of dynamic angular animations using AHM and funneling effects. We address this gap by comparing these two tactile illusions in the context of 1D circular animations around the wrist.

III. EXPERIMENTAL METHODOLOGY

In this study, we address the research question of how AHM and Funneling effects compare in their ability to create tactile animation illusions on a circular display. We also investigate which parameters influence the perception of these illusions, including animation speed, layout, and angular precision.

We present three user experiments. The first one focuses on the definition of new parameters for AHM to enable a comparison with funneling animations. The second one compares AHM and funneling for different animation speeds and layouts. With the last one, we establish Just Noticeable Differences (JND) values for different angles rendered with a funneling effect.

A. Apparatus

We designed and implemented two different devices in order to compare two layouts studied in the literature [28]. With both layouts, we used four actuators as suggested by Niwa *et al.* [32]. With the *band* layout, the four actuators are spread equally around the wrist, similarly to [10], [11] (Figure 1a). The average human wrist size is 177 mm (5 %: 162 mm, 95 %: 193 mm) for male and 150 mm (5 %: 137 mm, 95 %: 162 mm) for female [31]. The space between two actuators is therefore

typically between 34 mm and 48 mm. In all the experiments, the participants were seated with the elbow of the arm wearing the device resting on a desk and the wrist up.

With the *watch* layout, the four actuators are placed on the top of the wrist, like the contact between a watch on a wrist in a cross layout (Figure 1b). The front and back actuators are separated by 28 mm, and the left and right actuators are separated by 41 mm.

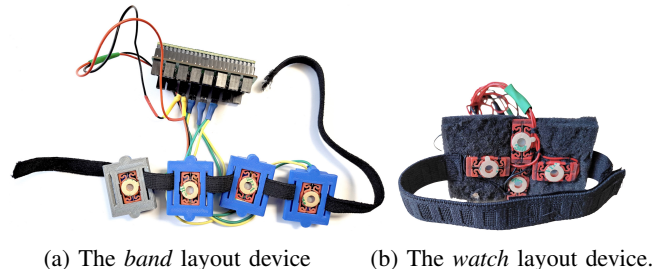(a) The *band* layout device   (b) The *watch* layout device.

Fig. 1: Devices used in the experiments.

Both devices use the same electronics. It uses a Teensy 4.1 microcontroller board that drives each actuator with a *frequency* modulated with an *amplitude* signal thanks to an *AND* gate. The *frequency* signal is a square signal up to 65 kHz, used up to 1000 Hz in practice. The *amplitude* signal is a high-frequency square signal of 31 kHz, the amplitude of actuation being controlled with the duty cycle of this signal with a 256-levels precision. The actuators are HiWave Haptic Exciter (HIHX9C005-8), 26 mm long and 12 mm wide. The actuated part is a circle of 11 mm diameter.

B. Funneling model

The funneling effect or phantom illusion creates the sensation of feeling a vibration between two tactile stimulations (Figure 2). To create this effect, we interpolate the amplitude of actuation of the two actuators surrounding the desired location of the phantom vibration with Gupta *et al.*'s formulas [10]. The parameter of Funneling animations is Revolution Duration (RD), which represents the duration of a 360° animation and its direction.
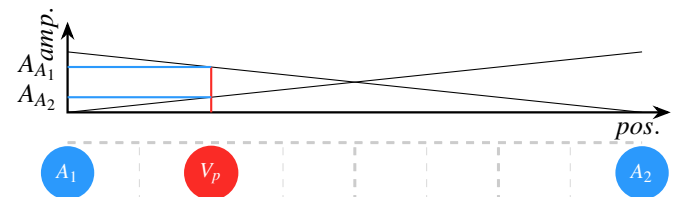

Fig. 2: Funneling effect, or phantom illusion, with a linear model. A phantom vibration V_p is created between two actuators A_1 and A_2. The amplitude of actuation of A_1 and A_2 is proportional to the distance to V_p.

The actuation signals of the funneling illusion are bijections between the position of the phantom vibration and the amplitude of actuation (Figure 2). Therefore, the resolution *res* of Funneling displays depends on the number of actuators n and the sampling rate of the amplitude signal r, and is given by:

$$res(n, r) = n \times r \qquad (1)$$

In our case $n = 4$ and $r = 256$ gives $r = 1024\,\text{pt}/360°$.

C. Apparent Haptic Motion

The first tactile animation illusion is Apparent Haptic Motion (AHM). We adapted this concept to a circular display as depicted on Figure 3. Instead of the usual *Stimuli Onset Asynchrony* (SOA) and *Duration of Signals* (DoS), we design a couple of parameters that describe both the spatial and temporal aspects of the animation, allowing an easier comparison of AHM to the Funneling model above. To this end, we used RD as a common parameter with funneling animations. The other parameter *Angle per Actuator* (APA) enables a full compatibility with SOA and DoS. It corresponds to the size of the zone of activation of each actuator. Since we use four actuators, the APA values must be between 90° and 180° to make sure the zone of activation of each actuator overlaps with the zone of activation of the two adjacent actuators, but not with the opposite actuator.
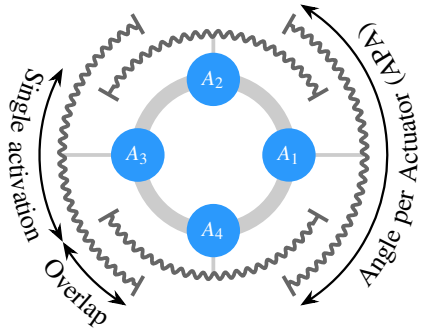

Fig. 3: Zone of activation of each actuator on the circular display. APA values are chosen so that the zone of activation of each actuator overlaps with the zone of actuation of the previous and next one. In this example, the APA is 120°.

SOA and DoS can be computed directly from *APA*, *RD*, and the number of actuators n as described by equations 2 and 3 below. We notice that SOA is proportional to the animation speed because it only depends on *RD*. However, DoS depends on both spatial (*APA*) and animation speed (*RD*) parameters. Hence the difficulty in designing animations with these parameters. With our new parameters, we intend to facilitate the design of tactile animations.

$$DoS = \frac{RD \times APA}{360} \quad (2) \qquad SOA = \frac{RD}{n} \quad (3)$$

Considering the AHM effect requires overlaps between consecutive signals, the resolution of an AHM display only depends on the number of actuator n because there are n overlap zones and n single activation zones. Hence:

$$res(n) = 2 \times n \qquad (4)$$

In our case, $n = 4$, hence the resolution of our display is $r = 8\,\text{pt}/360°$. The Figure 4 depicts the temporal sequence of activation of each actuator, and the correspondence with *SOA* and *DoS*. As a reference to other works, the TABLE I shows

the *SOA* and *DoS* values corresponding to the *APA* and *RD* values used in the experiments below.
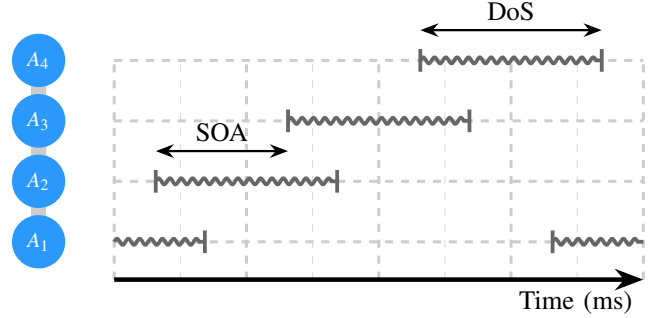

Fig. 4: Timeline showing the actuation sequence for a 360° animation with a constant speed.

TABLE I: SOA and DOS values in ms depending on RD and APA values used in the experiments below, with 4 actuators.

		RD							
		90	180	270	360	450	540	630	720
APA	**105**	26	53	79	105	131	158	184	210
	120	30	60	90	120	150	180	210	240
	135	34	68	101	135	169	203	236	270
	150	38	75	113	150	188	225	263	300
	165	41	83	124	165	206	248	289	330
SOA		23	45	68	90	113	135	158	180

Funneling displays have a higher resolution than AHM displays. Moreover, their animation effect is generated through spatial summation, in contrast to the temporal summation employed by AHM. Hence, unlike AHM, Funneling animations allow for variable speed animations, which can pause or even move back. Therefore with the Funneling model, it is possible to represent a vibration that the user can move around continuously [10]. This is why AHM is most suited for non-interactive animations. Therefore, in the three studies below we focus on non-interactive animations.

These studies were approved by the Inria's ethics board (decision 2022-37). Each study lasted approximately 30 min. The participants were instructed to complete the task at their own pace, as response time was not measured.

IV. EXPERIMENT I: CHOOSING A SUITABLE APA

In order to compare the performance of AHM and funneling, we first need to reduce the two models to the same set of parameters. With both models, we can adjust *RD*, but *APA* is specific to AHM. Therefore this first experiment is a pilot study to identify the best value for *APA*, and quantify the difficulty to interpret tactile animation illusions depending on *RD*. Consistent with previous studies in the literature, we consider the interpretation of the animation direction as an indicator of participants' ability to interpret tactile animation illusions [20].

Our hypothesis first H_1 is that *APA* values that lead to undistinct overlaps will make it harder to interpret the animation. Hence, we expect a sweet spot value that we would like to use in the next experiment.

Our second hypothesis H_2 is that the faster the animation (lower *RD* value) the harder it will be for participants to interpret the animation.

A. Methodology

We recruited 16 participants from the local laboratory and university, as well as acquaintances (10 male, 6 female). They were aged between 20 and 41 (*mean* = 27). One of the participants was self-reported left-handed, and all the others were self-reported right-handed.

The participants were seated on a chair in front of the computer used to display the experimental application (Figure 5). The experimenter attached the device around the wrist of their non-dominant hand. The experimenter made sure the actuators were spaced equally, and that they were not too close to the wrist bone to avoid conduction of the vibration through the bones. Then the experimenter explained to the participants the tasks and asked them to sign an informed consent form. During the experiment, the participants wore a noise-canceling headset to avoid audio cues. In each trial, the participants could feel the stimulus only once.
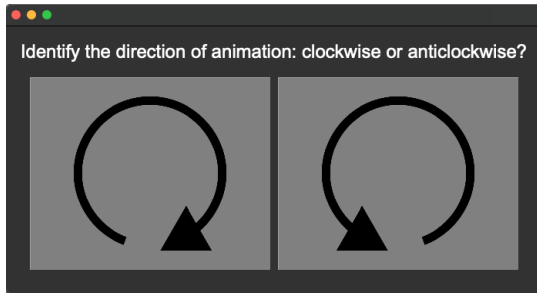

Fig. 5: Screenshot of the Experiment I application.

To investigate these hypotheses, we designed a simple task consisting of presenting participants 360° AHM animations either clockwise or anticlockwise. In each trial, we asked the participants which direction of animation they felt between *clockwise* and *anticlockwise*. As depicted on Figure 5, we displayed arrows on the clockwise and anticlockwise buttons to avoid any confusion due to language interpretation. We used the ratio of correct answers as a measure of the participants' ability to interpret the animations correctly, similarly to [32], [34]. The experiment follows a 2-Alternative Forced Choice (2AFC) protocol, in which a 50 % correct response rate is expected when participants are unable to identify the direction of the animation. We experimented several APA values to study H_1 and several RD values to study H_2.

The experiment followed a within-subject design with factors APA (105°, 120°, 135°, 150°, 165°); RD (90 ms/360°, 180 ms/360°, 270 ms/360°, 360 ms/360°, 450 ms/360°, 540 ms/360°, 630 ms/360°); 2 DIRECTIONS (clockwise, anticlockwise); and 3 REPETITIONS. The order of the trials was randomized to avoid any second-guess. The tactile cues were 360° AHM animation made of 250 Hz square signals. We used the *band* prototype for this experiment.

The total number of trials is: 5 APA × 7 RD × 2 DIRECTIONS × 3 REPETITIONS × 16 PARTICIPANTS = 3360 trials.

B. Results

1) Angle per Actuator (APA): Since each trial provided only a binary response, we aggregated the data by PARTICIPANT and APA to get a *Correct response rate* out of 35 trials. Visual analytics suggests no evidence that any APA value facilitates the recognition of the animation direction (Figure 6). The participants had a 50% chance of giving the right answer.

We analyzed this data with a linear regression and there is no significant impact on APA the *Correct response rate* ($b = 0.0003$, $t(3) = 0.56$, $p = 0.61$)Therefore, we fail to reject the null hypothesis, meaning this test gives no evidence that APA influences the recognition of animation direction. Further, the *Correct response rates* are all close to the mid-point between the chance rate and the maximum rate: 105° (75%), 120° (78%), 135° (78%), 150° (74%), and 165° (80%). We found that the intercept significantly predicts the *Correct response rate* ($a = 0.73$, $t(3) = 9.06$, $p < 0.002$). These results suggest that APA does not play a critical role in participants' ability to determine animation direction. Hence, we reject hypothesis H_1.
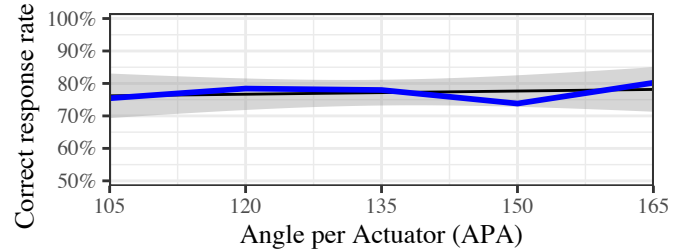

Fig. 6: Recognition rate per APA in the Experiment I. The blue curve is the average Correct response rate for all the tested APA. The black curve is the linear regression.

2) Revolution Duration (RD): To analyze both RD and direction, we consider the percentage of *Clockwise answers* per *Relative Revolution Duration* (*RRD*). RDD corresponds to the duration of a 360° animation in a given direction in ms. Trials with a positive *RRD* correspond to *clockwise* animations and trials with a negative *RRD* correspond to *anticlockwise* animations. According to our hypothesis H_2, we expect RDD values close to 0 to be difficult to interpret, hence a related percentage of *Clockwise answers* close to 50 %, the chance level. Similarly, we expect RDD values far from 0 to be easier to interpret, hence to reach closer to 100 % for positive RDD values (*clockwise* animations), and closer to 0 % for negative RDD values (*anticlockwise* animations). The 0 value is undefined since it corresponds to an infinite speed.

Visual analytics on Figure 7 suggests an effect of *RRD* on the percentage of *Clockwise answers*. We analyzed this data with a logistic generalized linear model regression. We observed a significant impact of *RRD* on the percentage of *Clockwise answers* ($\alpha = -0.325$, $\beta = 0.004$, $z = 30.4$, $p < 0.0001$), $f(x) = 1/(1 + e^{-(\alpha + \beta x)})$.

C. Discussion

We expected the *APA* to influence the users' ability to interpret AHM animations. However, our results contradicted
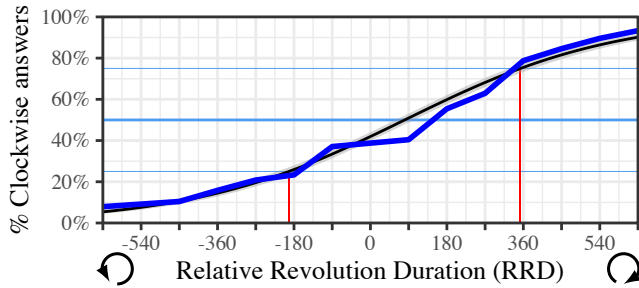
Fig. 7: Psychometric curve of the Experiment I. The blue curve is the collected data, and the black curve is the logistic regression.

this hypothesis. They suggest that APA does not affect *Correct response rate*, which is 75% for all the APA values, *i.e.* the mid-point between the chance rate and the maximum rate. Hence, we reject hypothesis H_1. Therefore, haptic animation designers can pick any *APA* value. Most importantly, this result suggests that when the APA value is set, controlling the animation speed only relies on one factor, *RD*. It enables an easier comparison between AHM and the funneling animations in the next studies. In our design rationale, we used *APA* values between $\frac{360}{n}$ and $\frac{720}{n}$, with n the number of actuators to cover the full circle with one or two actuators activated at the same time like other studies on AHM. However, further studies could characterize the effects of larger values that would enable more actuators activated at the same time and see if it improves AHM illusions.

Based on our results, we can reasonably accept hypothesis H_2 stating that faster animations are more difficult to interpret. Our model gives an threshold of non-detection of $192\,\mathrm{ms}/360°$ for *anticlockwise* animations and $353\,\mathrm{ms}/360°$ for *clockwise* animations. These values are similar to previous work with 6 ERM actuators that observed a correct interpretation rate above 75 % with speeds slower than $4\,\mathrm{cycles/s}$ ($250\,\mathrm{ms}/360°$) [34]. We experimented *RD* values ranging from a difficult value ($90\,\mathrm{ms}/360°$) to an easy value ($630\,\mathrm{ms}/360°$). Since the signals were 360° animations, the fastest animations lasted only 90 ms for a *DoS* down to 26 ms with a 105° *APA*. This condition was intentionally difficult in order to quantify the limits of perception. The slowest animations lasted 630 ms for a *DoS* up to 288 ms with a 165° *APA*, which is comparable to tactile animations in other studies [14], [15], [20]. We also notice an asymmetry of results between clockwise and anticlockwise answers. We think this is due to the asymmetry of the wrist, in particular the position of bones, muscles, and mechanoreceptors [43]. The wrist does not have a circular section like on our model 3. This assumption should be validated with future user studies, for example with stimulations on both the right and left wrists.

V. EXPERIMENT II: COMPARING METHODS AND LAYOUTS

This experiment has two objectives. The first one is to know if one of the two actuator layouts we designed facilitates the interpretation of tactile animation illusions. The second one is to compare the participants' ability to interpret *AHM* and *Funneling* animations.

In their experiment, Matscheko *et al.* observed that their participants identified better tactile animated patterns with the *band* layout than with the *watch* layout [28]. We expect to obtain similar results with tactile animation illusions. Therefore, our first hypothesis H_1 is that participants will interpret better the animations with the *band* layout than with the *watch* layout.

The *funneling* illusion gives continuous feedback as opposed to AHM which gives discrete feedback (8 zones on 360° with 4 actuators). Hence, our second hypothesis H_2 is that participants will interpret better the animations with the *funneling* method than with the *AHM* method.

A. Methodology

We recruited 20 participants from the local laboratory and university, as well as acquaintances (14 male, 6 female). They were aged between 16 and 50 (*mean* = 27). One of the participants was self-reported left-handed, and all the others were self-reported right-handed. None of the participants participated in the previous experiment.

The apparatus and procedure were the same as in the previous experiment. The main difference is that the two prototypes and the two animation methods were tested. The experimenter switched the devices on the participant's hand when necessary between the conditions.

This experiment uses a similar methodology than the previous one. However, in this experiment, the participants will perform 4 tasks: the combination of 2 METHODS (*funneling* and *AHM*), and 2 LAYOUTS (*band* and *watch*). The order of these 4 tasks was balanced between the participants, and they were allowed to take a break between the conditions. In each task, the participants performed 5 REPETITIONS of 2 DIRECTIONS and 9 RD ($90\,\mathrm{ms}/360°$, $180\,\mathrm{ms}/360°$, $270\,\mathrm{ms}/360°$, $360\,\mathrm{ms}/360°$, $450\,\mathrm{ms}/360°$, $540\,\mathrm{ms}/360°$, $630\,\mathrm{ms}/360°$, $720\,\mathrm{ms}/360°$, $810\,\mathrm{ms}/360°$). The signals used to create these tactile animation illusions are based on $250\,\mathrm{Hz}$ square signals. The tactile cues were a full revolution (360° angle) starting at 0°, which is the top actuator with the *band* layout and the forward actuator with the *watch* layout. We used a 120° APA for the *AHM* model, therefore the overlaps between zones of activation were 30° on both sides and the zones of single activation were 60° (Figure 3).

The total number of trials is: 2 METHODS × 2 LAYOUTS × 9 RD × 2 DIRECTIONS × 5 REPETITIONS × 20 PARTICIPANTS = 7200 trials.

B. Results

A logistic regressions shows that RRD has a significant impact on the *percentage of clockwise answers* ($\alpha = -0.131$, $\beta = 0.003$, $z = 43.28$, $p < 0.001$). We further analyzed the impact of RRD on the *percentage of clockwise answers* for each condition (Figure 8). The TABLE II shows the results of the logistic regressions of RRD on the *percentage of clockwise answers* for each of the 4 conditions, as well as the intervals

of non-detection (25% and 75%) thresholds based on the resulting models. These analyses reveal a significant effect for all the conditions.

TABLE II: Logistic regression statistics for both tactile animation illusions and both actuator layouts. Threshold values are means with 95% confidence intervals.

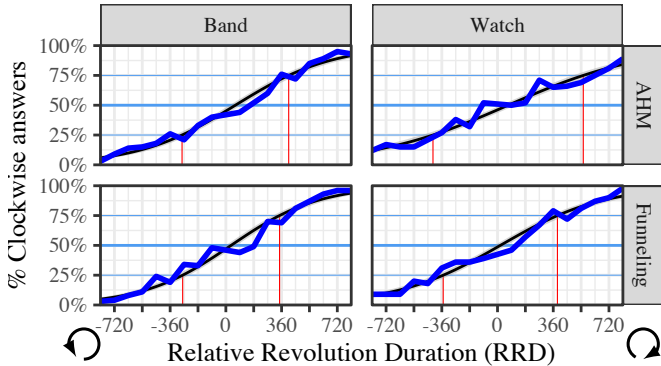| Method	Layout	α	β	z	p	Th$_{25}$	Th$_{75}$
AHM	Watch	-0.155	0.002	19.04	<0.001	-417 (±154)	554 (±167)
Funneling	Watch	-0.054	0.003	21.77	<0.001	-351 (±90)	387 (±119)
AHM	Band	-0.196	0.003	22.24	<0.001	-283 (±85)	406 (±97)
Funneling	Band	-0.118	0.003	22.89	<0.001	**-279 (±80)**	**347 (±84)**

Fig. 8: Psychometric curves for both tactile animation illusions and both actuator layouts. The blue curves show the collected data and the black curves are the logistic regressions

We observe that the *Funneling + band* condition has the smallest interval of non-detection, and that the *AHM + watch* layout has the largest. The Figure 9 figure further shows the 95% intervals for the 25% (anti-clockwise) and 75% (clockwise) thresholds for both METHOD and LAYOUT. We notice that the results of the previous experiment fit within the confidence intervals of the AHM+Band condition. We computed the logistic regression for each PARTICIPANT, METHOD, and LAYOUT to compute the anticlockwise and clockwise thresholds for each of the combinations of these three factors.
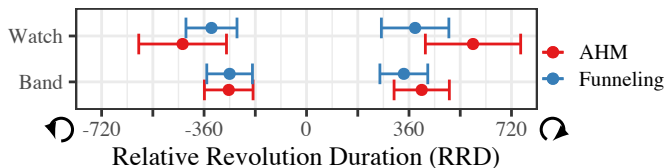

Fig. 9: 25% (anti-clockwise) and 75% (clockwise) thresholds for each conditions with 95% confidence intervals.

Then, we ran two-way repeated-measure ANOVAs on both these anti-clockwise and clockwise thresholds. The results of the Shapiro-Wilk normality tests for the residuals from both thresholds indicated no significant deviation from normality ($p = 0.7$ and $p = 0.3$, respectively), suggesting that the assumption of normality was met for our ANOVA analysis. We did not detect significant effects of METHOD ($F_{1,19} = 2.6$, $p = 0.12$), nor LAYOUT ($F_{1,19} = 2.8$, $p = 0.11$), nor interaction

between METHOD and LAYOUT ($F_{1,19} = 2.5$, $p = 0.13$) on the anti-clockwise threshold. However, we found a significant effect of METHOD ($F_{1,19} = 14.8$, $p < 0.001$, $\eta_G^2 = 0.065$) but no effect of LAYOUT ($F_{1,19} = 1.9$, $p = 0.18$) on the on the clockwise threshold. We also found an interaction between METHOD and LAYOUT ($F_{1,19} = 6.7$, $p < 0.02$, $\eta_G^2 = 0.019$) on the clockwise threshold. We conducted a pairwise t-test with a Bonferroni correction between the four conditions on the clockwise threshold and the only significant difference is between *Funneling + Band* and *AHM + Watch* (TABLE III).

TABLE III: Post-hoc analysis of the clockwise detection threshold.

	AHM+Band	AHM+Watch	Funneling+Band
AHM+Watch	0.18	-	-
Funneling+Band	1.00	**0.02**	-
Funneling+Watch	1.00	0.09	1.00

C. Discussion

Taken together, these results give evidence that the tactile animation illusions are easier to interpret with the *band* layout than with the *watch* layout. However, we only observed this difference in the *clockwise direction* with the *AHM* method. Hence, we partially validate H_1, which extends previous work on tactile animations [28].

The interaction between METHOD and LAYOUT suggests that the LAYOUT effect is essentially due to the difficulty of interpreting tactile animation illusions with *AHM* on the *watch* layout. This is weak evidence that *AHM* illusions are more complex to interpret in some cases than *funneling* illusions. However, with the *band* layout the performance of both *methods* are similar. Hence, we partially validate H_2 with the *watch* layout, but not with the *band* layout.

More studies are necessary to draw definitive conclusions. We designed a compact layout because we assumed that watches have space constraints. However, larger layouts may lead to better results with the watch layout. The asymmetry of the results is not as large as in the previous experiment. Further studies would be necessary to identify the factors that affected this result as suggested in the previous section.

VI. EXPERIMENT III: ANGLE JND

The first two experiments used 360° animations. However, the users may want to represent other angles. Therefore, in this experiment, we investigate the precision with which users can discriminate different angular extents of tactile animations by measuring their Just Noticeable Difference (JND) for angles between 0° and various reference angles.

With both methods, the users can leverage the duration of the signal to estimate the angle value. However, both methods provide additional cues to help users to estimate the angle, based on the display resolution as described in section III: up to 1024 pt/360° for Funneling and 8 pt/360° for AHM. It represent an angular precision of 0.35° per point for Funneling and 45° for AHM.

We anticipate that the precision at which users can distinguish funneling tactile animation illusions lies between these

two values. Gupta et al. measured a mean threshold of 19.1 sections on a 360° tactile display with direct manipulation, which leads to 18.8° precision [10]. In this experiment, the participants will feel the animation passively. Hence, we expect the task to be more difficult than with direct manipulation.

A. Methodology

We recruited 32 participants from the local laboratory and university, as well as acquaintances (12 male, 20 female). They were aged between 16 and 50 (*mean* = 24). One of the participants was self-reported left-handed, and all the others were self-reported right-handed. None of the participants participated in the previous experiments.

The participants were seated on a chair in front of the computer used to display the experimental application (Figure 10). Since the *band* layout got the best results in the previous experiment, we used this prototype for this experiment. The experimenter attached the device around the wrist of their non-dominant hand. The experimenter made sure the actuators were spaced equally, and that they were not too close to the wrist bone to avoid conduction of the vibration through the bones. Then the experimenter explained to the participants the tasks and asked them to sign an informed consent form. During the experiment, the participants wore a noise-canceling headset to avoid audio cues. In each trial, the participants could feel each of the three stimuli as described below only once by clicking on three buttons in a sequence. Only one button was active at a time. After the stimulus the next button was activated and after the last stimulus was played the participant had to indicate "Which animation feels shortest" (Figure 10).
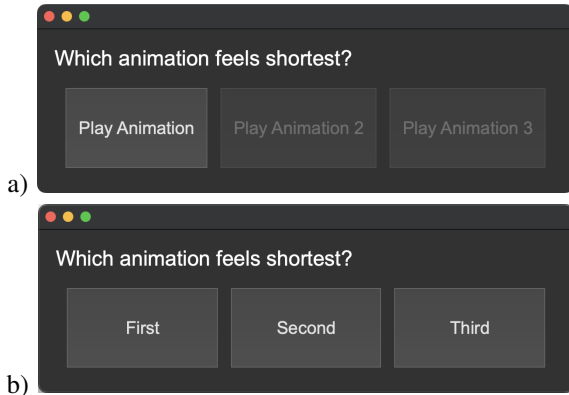
Fig. 10: Screenshots of the Experiment 3 application. a) the stimulus window; b) the answer window.

We used a one-up two-down adaptive procedure [25] with a 3-Alternative Forced Choice (3AFC) method to establish the JND for four REFERENCE ANGLES: 90°, 180°, 270°, and 360°. This means that two of the three stimuli were longer than the third stimuli by *delta* degrees. The *delta* between the reference angle and the two wrong answers started at 90°, decreased or increased by 10° increments depending on the correctness of the answers until the 4th reversal, then by 5° increments, until the 13th reversal, after which the task ended. This protocol is typically used to converge quickly towards the perception threshold [24]. All the trials used anticlockwise

animations with $RD = 720\,\text{ms}/360°$ based on 250 Hz square signals. According to Experiment II, participants should be able to interpret tactile animation illusions with this RD value.

We analyzed the *delta* values at the last 10 REVERSALS of each run, which correspond to data points approximating the perception threshold. The experiment followed a mixed design with METHOD as a between-subjects factor, and REFERENCE ANGLES as a within-subject factor. The order of REFERENCE ANGLES was balanced between the participants. Therefore, the following analysis is based on (16 PARTICIPANTS × 2 METHODS) × 4 REFERENCE ANGLES × 10 REVERSALS = 1280 trials.

B. Results

The Figure 11 shows the mean *JND* values and the linear regressions for each of the four *reference angles* with 95% confidence intervals for both the *AHM* and *Funneling* METHODS. We analyzed this data with a linear regression. The APA and intercept significantly predicts the *JND* for both *Funneling* ($b=0.18$, $t(2)=34.5$, $p<0.001$) and *AHM* ($b=0.12$, $t(2)=10.3$, $p<0.01$) and the intercept as well for *Funneling* ($a=23.14$, $t(2)=17.3$, $p<0.003$) and *AHM* ($a=25.94$, $t(2)=9.2$, $p<0.01$). The overall model predicts the *JND* very well for both *Funneling* (*adjusted* $R^2=0.99$, $F(1,2)=1190$, $p=0.001$) and *AHM* (*adjusted* $R^2=0.98$, $F(1,2)=107$, $p=0.01$). Hence, we describe the JND as a function of the reference angle for both the AHM and Funneling methods as follows:

$$\Delta A_F = 23.14 + 0.18A \quad (5) \quad \Delta A_{AHM} = 25.94 + 0.12A \quad (6)$$
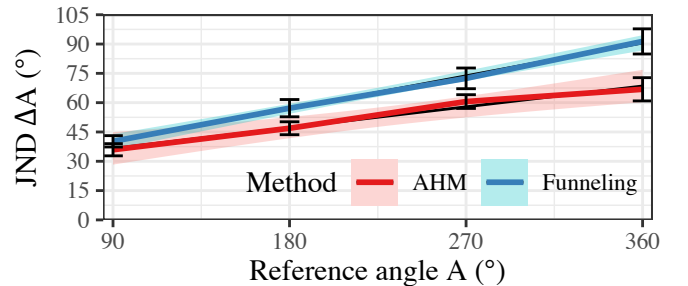
Fig. 11: JND values for tactile animation illusions with a funneling effect for four reference angles: 90°, 180°, 270°, and 360°. The error bars indicate 95% confidence intervals.

We also analyzed the results with a Two-Way ANOVA. A Mauchly' test for sphericity shows that we cannot assume sphericity for REFERENCE ANGLE ($W(3)=0.69$, $p=0.03$) and for the interaction between METHOD and REFERENCE ANGLE ($W(3)=0.69$, $p=0.03$). Therefore, we applied Huynh-Feldt corrections ($\varepsilon=0.82$) to the following results for REFERENCE ANGLE and the interaction between METHOD and REFERENCE ANGLE. We observed a significant difference between REFERENCE ANGLES ($F_{2.73,95.55}=24.3$, $p<0.0001$, $\eta_G^2=0.22$). We did not observe a significant difference between METHODS ($F_{1,35}=0.1$, $p>0.05$), nor a significant interaction between METHOD and REFERENCE ANGLE ($F_{2.73,95.55}=0.2$, $p>0.05$).

C. Discussion

The linear regressions show that the JND follows Weber's law for both *Funneling* and *AHM* for reference angles between 90° and 360°. Interestingly, the JND values for *AHM* vary between 36° and 67°, which is similar to the Overlap angle (30°) and the Single activations angle (60°). In a similar way, the JND values for *Funneling* vary between 40° and 91°. These results suggest that the perception is linked to the theoretical precision of these tactile animation illusions.

Further studies are necessary to establish causality though. To investigate this, future work should study the angle discrimination threshold of *AHM* with different *APA* values, hence different Overlap and Single activation values.

Moreover, it would be interesting to know if the linear relation stands with larger values or if it plateaus around the maximum theoretical resolution for both *AHM* and *Funneling*. It would also be interesting to know the relation between smaller reference angles and the JND, as the intercept is greater than zero.

VII. Conclusion

The *Stimuli Onset Asynchrony* (SOA) and *Duration of Signals* (DoS) are the typical parameters used in the literature to describe AHM animations. However, they only describe the temporal aspect of animations, not the spatial aspects. We proposed new parameters for describing AHM animations on a circular display: the *Angle per actuator* (APA), a spatial parameter, and the *Revolution duration* (RD), a spatiotemporal parameter. In our first user study, we showed that people can interpret AHM regardless of the APA value. In our third study, we noticed that the APA value influences the theoretical resolution of the display because of the position of stimulus changes. However, further studies are required to know if it affects the angle discrimination threshold.

The user studies one and two also provided insights about the most appropriate RD to facilitate the interpretation of AHM and Funneling animations. Indeed, too fast animations are too difficult to interpret, hence we recommend at least 360 ms/360°. We also noticed an asymmetry in the results to some extent. Further studies are necessary to assess if this effect is due to the asymmetrical shape and structure of the wrist.

In our third experiment, we only studied the angle discrimination thresholds for reference angles between 90° and 360°. It would be interesting to study smaller and larger values to know the contribution of the theoretical resolution of these tactile animation illusions on these thresholds. Further, the reference angles we used were at the location of the actuators, where the stimulation is unique and the strongest. It would be interesting to study the angle detection threshold for intermediate positions as well.

Our prototype has four actuators, which seemed sufficient for providing enough resolution and expressivity while keeping a simple design [2], [10], [11], [28]. Other studies in the literature preferred using more actuators [17], [50], typically with less accurate actuators (ERM or LRA). Our theoretical analysis shows the relationship between the number of actuators and the theoretical resolution of AHM and Funneling animations. Experimenting with prototypes with more actuators, like [34] would be another way to study the connection between the theoretical resolution and the angle discrimination threshold.

Last, in our studies we only studied perception thresholds and precision. We did not investigate the subjective aspects of tactile animation, like the sensation of continuity and smoothness. This is another avenue for future research in this field.

References

[1] D. S. Alles, "Information transmission by phantom sensations," *IEEE Transactions on Man-Machine Systems*, vol. 11, no. 1, pp. 85–91, 1970. DOI: 10.1109/TMMS. 1970.299967.

[2] J. Alvina, S. Zhao, S. T. Perrault, M. Azh, T. Roumen, and M. Fjeld, "Omnivib: Towards cross-body spatiotemporal vibrotactile notifications for mobile phones," in *Proceedings of the ACM Conference on Human Factors in Computing Systems (CHI)*, Seoul, Republic of Korea, 2015, pp. 2487–2496. DOI: 10.1145/2702123.2702341.

[3] A. Barghout, J. Cha, A. El Saddik, J. Kammerl, and E. G. Steinbach, "Spatial resolution of vibrotactile perception on the human forearm when exploiting funneling illusion," in *Proceedings of the IEEE International Workshop on Haptic Audio visual Environments and Games (HAVE)*, 2009, pp. 19–23. DOI: 10.1109/HAVE. 2009.5356122.

[4] G. von Békésy, "Neural volleys and the similarity between some sensations produced by tones and by skin vibrations," *The Journal of the Acoustical Society of America*, vol. 29, no. 10, pp. 1059–1069, 1957. DOI: 10.1121/1.1908698.

[5] G. von Békésy, "Funneling in the nervous system and its role in loudness and sensation intensity on the skin," *The Journal of the Acoustical Society of America*, vol. 30, no. 5, pp. 399–412, 1958. DOI: 10.1121/1.1909626.

[6] H. Burtt, "Tactual illusions of movement," *Journal of Experimental Psychology*, vol. 2, no. 5, pp. 371–385, 1917. DOI: 10.1037/h0074614.

[7] J. Cha, L. Rahal, and A. El Saddik, "A pilot study on simulating continuous sensation with two vibrating motors," in *IEEE International Workshop on Haptic Audio visual Environments and Games*, Ottawa, ON, Canada, 2008, pp. 143–147. DOI: 10.1109/HAVE.2008. 4685314.

[8] M. Eid, G. Korres, and C. B. F. Jensen, "SOA thresholds for the perception of discrete/continuous tactile stimulation," in *Proceedings of the International Workshop on Quality of Multimedia Experience (QoMEX)*, IEEE, 2015, pp. 1–6. DOI: 10.1109/QoMEX.2015.7148081.

[9] F. A. Geldard and C. E. Sherrick, "The cutaneous "rabbit": A perceptual illusion," *Science*, vol. 178, no. 4057, pp. 178–179, 1972. DOI: 10.1126/science.178.4057.178.

[10] A. Gupta, T. Pietrzak, N. Roussel, and R. Balakrishnan, "Direct manipulation in tactile displays," in *Proceedings of the ACM Conference on Human Factors in Computing Systems (CHI)*, San Jose, USA, 2016, pp. 3683–3693. DOI: 10.1145/2858036.2858161.

[11] A. Gupta, T. Pietrzak, C. Yau, N. Roussel, and R. Balakrishnan, "Summon and select: Rapid interaction with interface controls in mid-air," in *Proceedings of the ACM International Conference on Interactive Surfaces and Spaces (ISS)*, Brighton, UK, 2017, pp. 52–61. DOI: 10.1145/3132272.3134120.

[12] T. Hachisu and K. Suzuki, "Tactile apparent motion through human-human physical touch," in *Proceedings of EuroHaptics 2018*, Springer, 2018, pp. 163–174. DOI: 10.1007/978-3-319-93445-7_15.

[13] J. Hong, L. Stearns, J. Froehlich, D. Ross, and L. Findlater, "Evaluating angular accuracy of wrist-based haptic directional guidance for hand movement.," in *Graphics Interface*, 2016, pp. 195–200.

[14] A. Israr and I. Poupyrev, "Control space of apparent haptic motion," in *Proceedings of the IEEE World Haptics Conference (WHC)*, Istanbul, Turkey, 2011, pp. 457–462. DOI: 10.1109/WHC.2011.5945529.

[15] A. Israr and I. Poupyrev, "Tactile brush: Drawing on skin with a tactile grid display," in *Proceedings of the ACM Conference on Human Factors in Computing Systems (CHI)*, Vancouver, BC, Canada, 2011, pp. 2019–2028. DOI: 10.1145/1978942.1979235.

[16] S. Kasaei and V. Levesque, "Effect of vibration frequency mismatch on apparent tactile motion," in *Proceedings of the IEEE Haptics Symposium (HAPTICS)*, 2022, pp. 1–6. DOI: 10.1109/HAPTICS52432.2022.9765602.

[17] O. B. Kaul, M. Rohs, B. Simon, K. C. Demir, and K. Ferry, "Vibrotactile funneling illusion and localization performance on the head," in *Proceedings of the ACM Conference on Human Factors in Computing Systems (CHI)*, Honolulu, HI, USA, 2020, pp. 1–13. DOI: 10.1145/3313831.3376335.

[18] J. H. Kirman, "Tactile apparent movement: The effects of interstimulus onset interval and stimulus duration," *Perception & Psychophysics*, vol. 15, no. 1, pp. 1–6, 1974. DOI: 10.3758/BF03205819.

[19] L. Kohli, M. Niwa, H. Noma, K. Susami, Y. Yanagida, R. W. Lindeman, K. Hosaka, and Y. Kume, "Towards effective information display using vibrotactile apparent motion," in *Proceedings of the IEEE Haptics Symposium (HAPTICS)*, 2006, pp. 445–451. DOI: 10.1109/HAPTIC.2006.1627115.

[20] I. Lacôte, D. Gueorguiev, C. Pacchierotti, M. Babel, and M. Marchal, "Speed discrimination in the apparent haptic motion illusion," in *Proceedings of Eurohaptics*, Springer, 2022, pp. 48–56. DOI: 10.1007/978-3-031-06249-0_6.

[21] I. Lacôte, C. Pacchierotti, M. Babel, M. Marchal, and D. Gueorguiev, ""tap stimulation": An alternative to vibrations to convey the apparent haptic motion illusion," in *Proceedings of the IEEE Haptics Symposium (HAPTICS)*, 2022, pp. 1–6. DOI: 10.1109/HAPTICS52432.2022.9765620.

[22] S. Lavenant, A. Goguey, S. Malacria, L. Nigay, and T. Pietrzak, "Study of the perception of vibrotactile haptic cues on the fingers hand and forearm for representing microgesture," in *Proceedings of the IEEE International Symposium on Mixed and Augmented Reality (ISMAR)*, Bellevue, Washington, USA, 2024. DOI: 10.1109/ISMAR62088.2024.00092.

[23] S. J. Lederman and L. A. Jones, "Tactile and haptic illusions," *IEEE Transactions on Haptics*, vol. 4, no. 4, pp. 273–294, 2011. DOI: 10.1109/TOH.2011.2.

[24] M. R. Leek, "Adaptive procedures in psychophysical research," *Perception & Psychophysics*, vol. 63, pp. 1279–1292, 2001. DOI: 10.3758/BF03194543.

[25] H. Levitt, "Transformed up-down methods in psychoacoustics," *The Journal of the Acoustical Society of America*, vol. 49, no. 2B, pp. 467–477, Feb. 1971. DOI: 10.1121/1.1912375.

[26] Z. Liao, J. V. S. Luces, and Y. Hirata, "Human navigation using phantom tactile sensation based vibrotactile feedback," *IEEE Robotics and Automation Letters*, vol. 5, no. 4, pp. 5732–5739, 2020. DOI: 10.1109/LRA.2020.3010447.

[27] G. Luzhnica, S. Stein, E. Veas, V. Pammer, J. Williamson, and R. M. Smith, "Personalising vibrotactile displays through perceptual sensitivity adjustment," in *Proceedings of the ACM International Symposium on Wearable Computers (ISWC)*, Maui, Hawaii, 2017, pp. 66–73. DOI: 10.1145/3123021.3123029.

[28] M. Matscheko, A. Ferscha, A. Riener, and M. Lehner, "Tactor placement in wrist worn wearables," in *Proceedings of the ACM International Symposium on Wearable Computers (ISWC)*, Seoul, South Korea, 2010, pp. 1–8. DOI: 10.1109/ISWC.2010.5665867.

[29] T. Moesgen, H.-N. Ho, and Y. Xiao, "Apparent thermal motion on the forearm," in *Proceedings of Eurohaptics 2024*, 2024, pp. 56–68. DOI: 10.1007/978-3-031-70058-3_5.

[30] B. J. Mortimer, G. A. Zets, and R. W. Cholewiak, "Vibrotactile transduction and transducers," *The Journal of the Acoustical Society of America*, vol. 121, no. 5, pp. 2970–2977, 2007. DOI: 10.1121/1.2715669.

[31] National Aeronautics and Space Administration, *NASA-STD-3000, Man-Systems Integration Standards, Volume I, Section 3: Anthropometry and Biomechanics*, https://msis.jsc.nasa.gov/sections/section03.htm, 1995.

[32] M. Niwa, R. W. Lindeman, Y. Itoh, and F. Kishino, "Determining appropriate parameters to elicit linear and circular apparent motion using vibrotactile cues," in *Proceedings of the IEEE World Haptics Conference (WHC)*, 2009, pp. 75–78. DOI: 10.1109/WHC.2009.4810856.

[33] M. Niwa, Y. Yanagida, H. Noma, K. Hosaka, and Y. Kume, "Vibrotactile apparent movement by dc motors and voice-coil tactors," in *Proceedings of the International Conference on Artificial Reality and Telexistence (ICAT)*, 2004, pp. 126–131.

[34] M. Ogrinc, I. Farkhatdinov, R. Walker, and E. Burdet, "Sensory integration of apparent motion speed and vibration magnitude," *IEEE Transactions on Haptics*, vol. 11, no. 3, pp. 455–463, 2018. DOI: 10.1109/TOH. 2017.2772232.

[35] S. Paneels, M. Anastassova, S. Strachan, S. P. Van, S. Sivacoumarane, and C. Bolzmacher, "What's around me? multi-actuator haptic feedback on the wrist," in *Proceedings of the IEEE World Haptics Conference (WHC)*, 2013, pp. 407–412. DOI: 10.1109/WHC.2013. 6548443.

[36] G. Park and S. Choi, "Tactile Information Transmission by 2D Stationary Phantom Sensations," in *Proceedings of the ACM Conference on Human Factors in Computing Systems (CHI)*, 2018, pp. 1–12. DOI: 10.1145/ 3173574.3173832.

[37] J. Park, J. Kim, Y. Oh, and H. Tan, "Rendering Moving Tactile Stroke on the Palm Using a Sparse 2D Array," in *Proceedings of EuroHaptics 2016*, Springer, 2016. DOI: 10.1007/978-3-319-42321-0_5.

[38] P. Patel, R. K. Ray, and M. Manivannan, "Power law based "out of body" tactile funneling for mobile haptics," *IEEE Transactions on Haptics*, vol. 12, no. 3, pp. 307–318, 2019. DOI: 10.1109/TOH.2019.2933822.

[39] S. T. Perrault, E. Lecolinet, J. Eagan, and Y. Guiard, "Watchit: Simple gestures and eyes-free interaction for wristwatches and bracelets," in *Proceedings of the ACM Conference on Human Factors in Computing Systems (CHI)*, 2013, pp. 1451–1460. DOI: 10.1145/2470654. 2466192.

[40] D. Pittera, O. Georgiou, and W. Frier, ""i see where this is going": A psychophysical study of directional mid-air haptics and apparent tactile motion," *IEEE Transactions on Haptics*, vol. 16, no. 2, pp. 322–333, 2023. DOI: 10.1109/TOH.2023.3280263.

[41] G. Richard, T. Pietrzak, F. Argelaguet, A. Lécuyer, and G. Casiez, "MultiVibes: What if your VR Controller had 10 Times more Vibrotactile Actuators?" In *Proceedings of the IEEE International Symposium on Mixed and Augmented Reality (ISMAR)*, 2023, pp. 703–712. DOI: 10.1109/ISMAR59233.2023.00085.

[42] D. Sadihov, B. Migge, R. Gassert, and Y. Kim, "Prototype of a VR upper-limb rehabilitation system enhanced with motion-based tactile feedback," in *Proceedings of the IEEE World Haptics Conference (WHC 2013)*, IEEE, 2013, pp. 449–454. DOI: 10.1109/WHC.2013. 6548450.

[43] J. V. Salazar Luces, K. Okabe, Y. Murao, and Y. Hirata, "A phantom-sensation based paradigm for continuous vibrotactile wrist guidance in two-dimensional space," *IEEE Robotics and Automation Letters*, vol. 3, no. 1, pp. 163–170, 2018. DOI: 10.1109/LRA.2017.2737480.

[44] O. S. Schneider, A. Israr, and K. E. MacLean, "Tactile animation by direct manipulation of grid displays," in *Proceedings of the ACM Symposium on User Interface Software and Technology (UIST 2015)*, 2015, pp. 21–30. DOI: 10.1145/2807442.2807470.

[45] C. E. Sherrick and R. Rogers, "Apparent haptic movement," *Perception & Psychophysics*, vol. 1, no. 3, pp. 175–180, 1966. DOI: 10.3758/BF03210054.

[46] Y. Singhal, D. Honrales, H. Wang, and J. R. Kim, "Thermal in motion: Designing thermal flow illusions with tactile and thermal interaction," in *Proceedings of the ACM Symposium on User Interface Software and Technology (UIST)*, 2024. DOI: 10.1145/3654777. 3676460.

[47] H. Tan, A. Lim, and R. Traylor, "A Psychophysical Study of Sensory Saltation With an Open Response Paradigm," in *Proceedings of the ASME International Mechanical Engineering Congress and Exposition (IMECE)*, Nov. 2000, pp. 1109–1115. DOI: 10. 1115/IMECE2000-2419.

[48] S. Ueda, M. Uchida, A. Nozawa, and H. Ide, "A tactile display using phantom sensation with apparent movement together," *Electronics and Communications in Japan*, vol. 91, no. 12, pp. 29–38, 2008. DOI: 10. 1002/ecj.10000.

[49] S. Weinstein, "Intensive and extensive aspects of tactile sensitivity as a function of body part, sex and laterality," in *The Skin Senses: Proceedings of the First International Symposium on the Skin Senses*, Thallahassee, Florida, 1968, pp. 195–222.

[50] K. Yatani and K. N. Truong, "Semfeel: A user interface with semantic tactile feedback for mobile touch-screen devices," in *Proceedings of the ACM Symposium on User Interface Software and Technology (UIST)*, 2009, pp. 111–120. DOI: 10.1145/1622176.1622198.

Thomas Pietrzak received a master's degree and a Ph.D. in computer science at the Université de Metz, France. He is currently a Full Professor at the Université de Lille, France, and a member of the Loki team, part of the CRIStAL (UMR 9189 CNRS) laboratory and the Inria Center of the Université de Lille. His research domain is Human-Computer Interaction, Haptics, and Virtual Reality. In particular, his research focuses on leveraging the human sensorimotor loop for the design of interaction techniques and interactive devices.

Rahul Kumar Ray received a master's Degree in biomedical engineering at the National Institute of Technology of Kurukshetra, India. He also obtained a Ph.D. in applied mechanics at the Indian Institute of Technology in Madras, India. He worked as a research engineer at the Inria Center of the Université de Lille. He is currently an assistant professor in FLAME University, Lavale, in Pune, India. His research interests are Haptics and Virtual reality engineering.